

GLOBAL JOURNAL OF ENGINEERING SCIENCE AND RESEARCHES
DEVELOPMENT OF ZrB₂-B₄C-Mo CERAMIC MATRIX COMPOSITE FOR HIGH
TEMPERATURE APPLICATIONS

Rajan Vedant^{*1}, Hari Parshad² & Priyanka Jain³

^{*1,2&3} Assistant Professor, Department of Mechanical Engineering, Ganga Technical Campus, Bahadurgarh

ABSTRACT

The present study deals with development of ceramic matrix composite containing the nominal compositions of three powders ZrB₂ (40 wt. %), B₄C (40 wt. %) and Mo (20 wt. %) were synthesized by ball milling and followed by conventional sintering in a furnace at 1500°C and 1600°C for 3 hours in presence of Ar gas and also spark plasma sintering at 1800°C for 1 min. During ball milling the crystallite size of the powder gradually decreases with increase in milling time from 0h to 60h and crystallite size of the final product reaches in submicron or Nano-metric level. The influence of the processing parameters on the phase evolution and chemical composition during ball milling, conventional sintering and spark plasma sintering for sub-micrometer or Nano-metric (60h milling) of the composites were investigated in detail by X-ray diffraction (XRD), scanning electron microscopy (SEM). The maximum densification of ZrB₂-B₄C-Mo ceramic matrix composite was achieved at 1800°C. The composites prepared by spark plasma sintering at 1800°C records extraordinary level of improvement of the hardness (27.34GPa) which is 3-4 times of higher hardness value than that of the composites sintered at conventional techniques. Similarly, the ball on disc wear resistant property of ZrB₂-B₄C-Mo ceramic matrix composite exhibits higher in the samples prepared by spark plasma sintering at 1800°C.

Keywords: *ZrB₂-B₄C-Mo ceramic matrix composite, Ball milling, X-ray diffraction (XRD), Scanning electron microscopy (SEM), Mechanical properties.*

I. INTRODUCTION

ZrB₂ is an ultra-high temperature ceramic with high melting point i.e. 3246°C, its hardness is more than the 500MPa. Over the last few years ZrB₂ceramic based composites are extensively used due to their best mechanical properties. It has superior electrical conductivity, corrosion resistance and also chemical stability against molten metal and non-basic slags [1-4].In view of these properties the main applications of ZrB₂ ceramic are in cutting tools, thermal protective systems, aero-crafts, crucibles which consist molten-metals and high temperature electrodes [5].

It is very difficult to make dense ZrB₂ materials at low temperature due to its high melting point and strong covalent-bonding. Densification of ZrB₂ involves usage of additives, without which the densification process will have to be carried out at high sintering temperatures of the order of 2100°C to 2300°C [6]. ZrB₂ ceramics have low fracture toughness 2.4 to 3.5 MPam^{1/2}and hence its applications are limited [7]. Therefore it is very important to develop a low-temperature process to produce ZrB₂ based ceramics with high toughness. To improve its fracture toughness researchers have added second phases like SiCp [8], SiCw[9], ZrSi₂[10] , ZrC[11], CNT[12] and B₄C[1]but it has been found that in most cases no improvement of fracture strength has been observed. Hence, improving both fracture toughness and strength of ZrB₂ based ceramics requires addition of some metal material. Also addition of metal material into these ceramics will result in improved densification even at low temperature [13, 14].

Among other ceramics such as diamond boron nitride, cubic boron nitride, B₄C (Boron carbide) occupies third position with respect to hardness and also abrasion resistance [15-17]. But at elevated temperatures (>13000C) B₄C has low density (2.52 g/cm³) and high hardness (35 to45GPa), so it is an ideal for applications requiring high temperature wear resistance. Other advantages of boron carbide include low cost, high neutron absorption ability, abundance of its raw material [18]. Zirconium di-boride (ZrB₂) and Boron carbide (B₄C) have interesting

properties, and by mixture of these two ceramics there is chance of covering each other's limitations related to physical and mechanical properties. Due to this reason, researchers have taken interest in examining the ZrB₂-B₄C composite. In recent years, work has been carried out such that any one of them was taken as matrix and another one taken as reinforcement. To consolidate ZrB₂-B₄C composite powders sintering techniques namely hot pressing, pressure-less sintering and microwave sintering are being used in recent years. Since, adding metal powders (such as Cr, Mo, W and Ni) improve densification of ZrB₂ based ceramics incorporating a third phase into ZrB₂-B₄C composite is necessary [13, 14]. Among these metals Molybdenum (Mo) was the choice of researchers because of its low density (10.2 g/cm³), high melting point (2610°C)[19] and low thermal expansion coefficient ($6 \times 10^{-6} \text{ K}^{-1}$), which is very close to that of ZrB₂ ($6.88 \times 10^{-6} \text{ K}^{-1}$)[20,21]. These properties make Mo suitable for low-temperature preparation of ZrB₂ based materials with high density and high fracture toughness. To the best of our knowledge, the sintering performance and properties of the ZrB₂-B₄C-Mo system have not been reported so far yet.

Objectives of the research work:

- (a) To synthesize ZrB₂-B₄C-Mo ceramic matrix composite by mechanical alloying and sintering (conventional and SPS).
- (b) To study the effect of sintering temperature on the ZrB₂-B₄C-Mo pellets.
- (c) Characterization of milled powders as well as sinter products by using XRD, SEM and EDS analyses.
- (d) To study of mechanical properties such as hardness and wear resistance of bulk ZrB₂-B₄C-Mo ceramic matrix composites.

II. LITERATURE REVIEW

2.1 Composite materials

The composite materials obtain from combining the two or more different materials to achieve desired properties that the each component cannot be attained by themselves.

2.2 Type of composite materials

1. Metal matrix composite (MMC)
2. Polymer matrix composite (PMC)
3. Ceramic matrix composite (CMC)

The aim of the developing Ceramic matrix composites (CMC) is to improve the ceramic desirable properties by incorporating reinforcements in them and limiting their inherent weaknesses. Development of CMCs imparts various improvements over ceramics such as:

- Capability of dynamic load is higher
- Degree of anisotropy on incorporation of fibers
- Improved fracture toughness
- Elongation to rupture up to 1%

2.3 Mechanically alloying:

Mechanical alloying (MA) is the solid-state powder processing technique which involves re-welding of powder particles, cold welding and fracturing in the high-energy ball milling. In mechanically alloying process a small amount of the blended powder mixture is put on the container along the grinder media such as stainless steel ball, zirconia ball and whole mass is agitated at a high speed for a predetermined length of time. Lubricant (also called process control agent) can be added occasionally, especially milling material is ductile. The Process control agent minimized the formation of the large lumps of powder and effect of cold welding. Alloying happens between the basic powders and homogeneous alloy is got toward the end of processing [22].

2.4 Processing of CMCs

Ceramic matrix composite materials can be produced by conventional sintering techniques utilized for making polycrystalline ceramic and also can be manufactured by new techniques such as spark plasma sintering, which is specifically for CMCs Making.[23]

2.4.1 Cold Pressing and Sintering

After the cold pressing of fiber and matrix powder, the green compact pellets followed by sintering are carried forward by conventional sintering processing of ceramic. Mostly in the sintering stage, the composite incurs lot of cracks due to the shrinkage of matrix. This shrinkage problem connected with the sintering of any type of ceramic. Few other problems arise when high-aspect ratio reinforcements are added to ceramic matrix material or a glass and attempted to sinter. Network formation takes place upon addition of whiskers and fibers, this network may restrict the sintering process. The difference in thermal expansion coefficients of matrix and reinforcement, may lead to hydrostatic tensile stress while cooling the matrix. The driving force for process of sintering gets affected by this hydrostatic tensile stress resulting in lower densification rate of the matrix [23]

2.4.2 Spark plasma sintering

Spark plasma sintering is a comparatively new technique that uses a pulsed direct current to heat the graphite pressure die and that allows very fast heating and cooling rates, short holding times and high pressures to obtain fully dense samples. In this newly developed technique of sintering the powders to be compacted are loaded in a die and a uniaxial pressure is applied while sintering (shown in Fig. 2.1). No use of external heating source is done in Spark plasma sintering. To heat the powder a pulsed direct current is allowed to pass through the electrically conducting die and the sample. In this process the die also acts as a heating source and the sample is heated from both inside and outside. Compaction of a wide variety of materials, e.g. functional graded materials, metals and alloys, composites and structural and functional ceramics are done by spark plasma sintering.

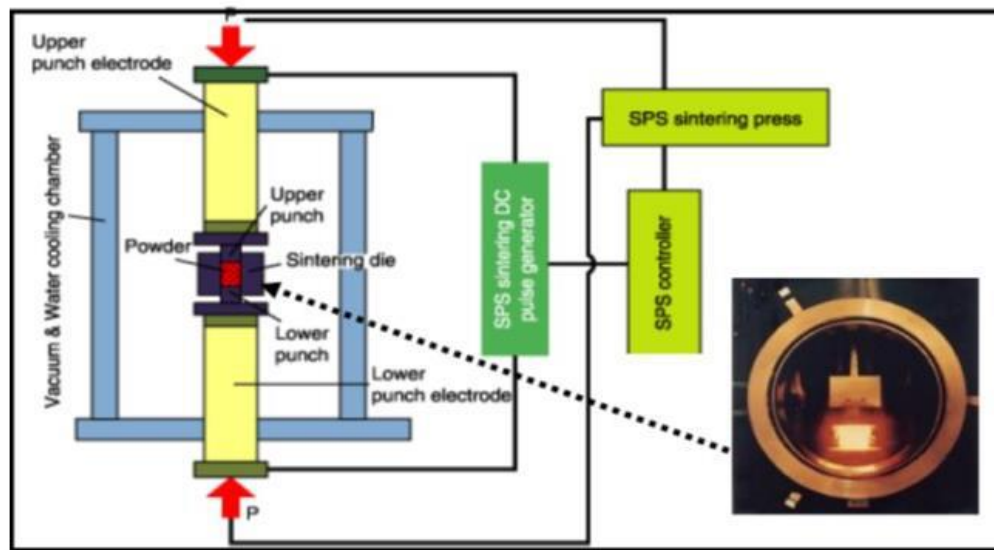


Fig. 2.1 Schematic diagram of spark plasma sintering

III. EXPERIMENTAL PROCEDURE

3.1 Synthesis of ZrB₂-B₄C-Mo ceramic composite

3.1.1 Powder Preparation:

The raw powders like ZrB₂ (ESK Ceramics GmbH & Co.Kg, Germany), boron carbide (Cerotech Trading Limited, Sanghai, China) and Molybdenum (Koch-Light Laboratories Ltd. UK) have a particle size 35 μ m, 20 μ m, 4 μ m respectively. Powders were the beginning material for synthesis by mechanical alloying. The alloy powder containing ZrB₂ (40 vol. %), B₄C (40 vol. %) and Mo (20 vol. %) are ball milled by utilizing zirconia ball media and toluene as grinding aid/coolant, at speed 350 rpm for 0 -60 hours. The green binder used in this process was PVA (Polyvinyl alcohol). There were three sets of powder synthesis, one alloy powder in micrometer size (avg. particle size \square 32 μ m) taken before mechanical milling, second alloy powder in sub-micrometer size-1 (average

particle size \square 20 μm) produced by 42 hours of milling and third alloy powder in sub-micrometer sized-2 (\square 12 μm) produced by 60 hours of milling.

3.1.2 Compaction:

Dry milled powders (all un-milled, 42h and 60h of milling) were mixed with binder named polyvinyl alcohol (PVA) to help strong compaction and to get bonding tendency. Each sample consists of 12g of milled powder mixed with the 4 ml of polyvinyl alcohol (PVA). The green compaction was done of binder mixed milled powders was carried out by using the single acting cylinder compaction machine (Fig. 3.1) with diameter of 9.5 mm at an applied pressure of 6 ton. The dwell time for each pressing was 120 s.



Fig.3.1: Single acting cylinder compaction machine.

3.1.3 Sintering

3.1.3.1 Conventional Sintering

The sintering of green compacts of sub-micrometer sized (60h of milling) size powders were carried out in a tubular furnace (Okay, Model no. 7017) (shown in Fig. 3.2) under the argon atmosphere. First tube was evacuated to a vacuum level of 10⁻⁵ bar and the specimens were placed on a crucible inside the chamber. All samples were sintered at 1500°C with holding time for 3 hours in Ar atmosphere.

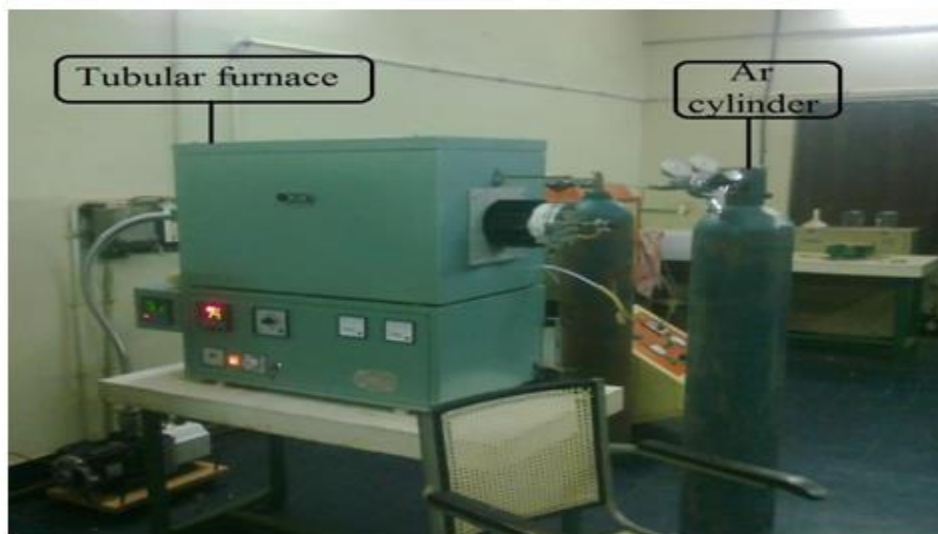


Fig.3.2: Tubular furnace is used for conventional sintering

3.1.3.2 Spark plasma sintering

Dry pellets of milled powder (60h) are placed on the bottom holding graphite plate by centering the pellet with respect to graphite rod attached to the system (shown in Fig. 3.3). The graphite rod is made in such way that it is hollow cylindrical in shape and the tip of the rod is connected by means of a small nozzle to provide atomizing behavior of argon gas during sintering process.



Fig. 3.3: spark plasma sintering equipment.

Following parameters are taken care during whole process and summarized in Table 3.1.

Table 3.1: Spark plasma sintering parameters

DC Voltage	20-40 Volt
Current	100-160Ampere
Argon rate	2.5litre/min
Sintering time	30sec-1min

To avoid oxidation behavior Argon will pass through continuously in the nozzle for 5 min after sintering. After constant flow of argon gas, reducing atmosphere was created around the pellet area to make proper sintering and avoiding oxidation behavior of the sample. Then according to above mention parameters sintering process carried out.

3.2 Microstructural characterization

3.2.1 X-ray diffraction

The different of milling time of powder sample (0h(un-milled), 42h,60h) and polished sintered composite at various sintering temperature were characterized through modal ULTIMA-IV XRD system (shown in Fig. 3.4) by utilizing Cu-K α ($\lambda=1.5418^\circ$) radiation to focus the phase evolution at various level of milling material and various sintering conditions. 20°-100°and 10°-60°range of scanning has been taken for scanning. And step size 5°/min has been taken.



Fig 3.4: XRD machine used for X-ray diffraction of the samples.

3.2.2 Scanning electron microscopy:

The microstructure of milled powder and sintered pellet observed by using of scanning electron microscopy (SEM, model-JSM 6480LV, make-JEOL) (shown in Fig. 3.5). Utilizing standard metallographic strategies all sample polished by mechanically before examination. Before examine sample coating has been done.



Fig 3.5: Scanning Electron Microscope (SEM) model-JSM 6480LV,make-JEOL

3.2.3 Optical Microscopy:

Fracture surfaces after ball on disc wear testing for sintered pellet at different temperature are observed by using optical microscope make-ZEISS, model- Axiocam ERc 5s (shown in Fig. 3.6).. In this optical the microstructures of ball on disc wear sample were analyzed with different magnification.



Fig 3.6: Optical microscopy with Image analyzer

3.3 Mechanical Testing

3.3.1 Vicker's Hardness measurement

Vickers's hardness tester is used on account of measurement of hardness. It has an indenter of square based pyramid of vertex angle 136° . It is also called the diamond-pyramid hardness test due to the shape of the indenter is diamond. Vickers hardness number is calculated by load divided by surface area of the indentation. VPH (Vickers's-pyramid hardness) number is calculated by using following equation:

$$VPH = \frac{2P \sin(\Theta/2)}{L^2}$$

Where L is the avg. length of diagonal in mm, P= applied load in Kg and Θ =angle in between opposite face of diamond as 136° . Hardness of sintered specimens was carried out using Vickers' Hardness Tester dwell time of 10 sec. and load of 1 kg. The crack is found at the corner of the indentation shown in Fig.

3.3.2 Wear study

Ball-on-plate wear tester (Ducom, TR-208 M1) machine (shown in Fig. 3.7) was used to performing the wear behavior of all the sintered pellets at different sintering temperature. The stainless steel ball in the dimension of 4 mm diameter rotates on the sintered pellet as shown in Fig 3.10 with the speed of 20rpm for 10 minutes under 20N constant load.



Fig 3.7: Ball-on- disc wear testing machine

IV. RESULTS AND DISCUSSIONS

4.1 X-Ray Diffraction (XRD) analysis:

4.1.1 XRD analysis of powders during milling

Fig.4.1a to c show that the X-ray diffraction spectrum of ZrB₂-B₄C-Mo milled powders taken at different time like 0h (un-milled), 40h and 60 h, respectively. It reveals that from the analysis of XRD pattern that intensity gradually decreases with increase of milling time. Also found with slightly increase in peak width with increase in milling time. The increment in peak width is because of introduce the lattice strain and decrease in particle size (avg. particle size reduce 32 μ m to 12 μ m). It is clear from the XRD patterns that the presence of ZrB₂, B₄C and Mo phases of each stage milling. For XRD analysis of milled powders at higher milling time (40h and 60 h) shows the peak shifting as well as peak gets broadening, this due to the fact micron-level powder gradually reduce their size into sub-micron or Nano-metric level due fragmentation of particles caused by high energy ball mill.

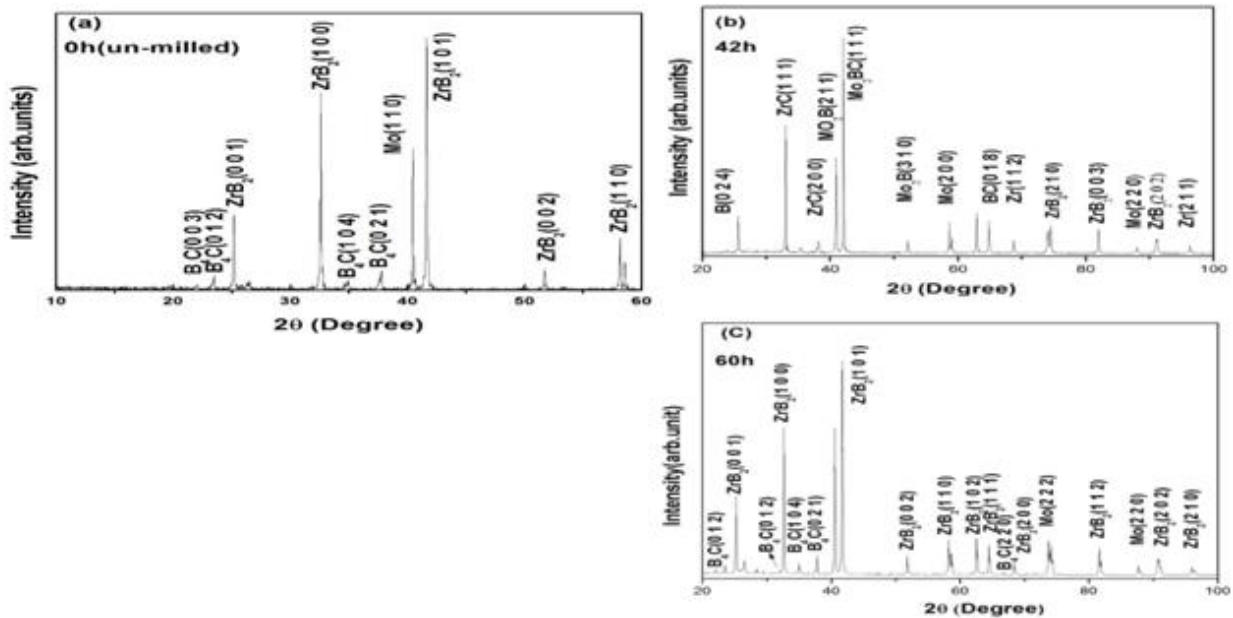


Fig. 4.1: XRD spectra of milled powders of ZrB₂-B₄C-Mo at different milling time: (a) 0h, (b) 42h and (c) 60h.

4.1.2. XRD analysis of sintered products

Fig. 4.2a and b show the XRD patterns of ZrB₂-B₄C-Mo composite sintered at 1500°C and 1600°C in a tube furnace in the presence of argon atmosphere for 3.0 hrs. It is evident that the presence of predominant phases like ZrB₂ and B₄C along with some intermetallic phases like MoB and Mo₂C/Mo₂BC in the sintered product. On the other hand, the XRD analysis of ZrB₂-B₄C-Mo composite sintered at 1800°C at plasma sintering technique for holding time of 30sec-1min (Fig.4.2c) shows similar kind of phases along with intermediate phases like ZrC, MoB, Mo₂B. but the XRD peaks show the broadening in nature. The reason behind this advanced sintering is that at very small holding time the grain growth is not possible.

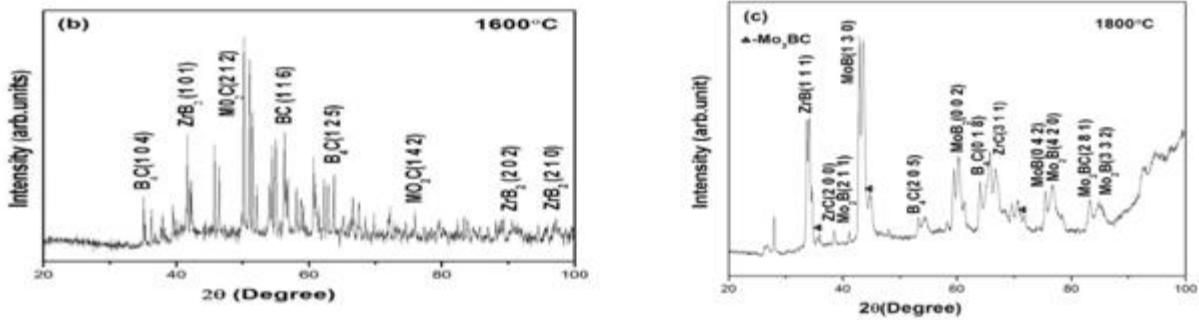


Fig 4.2: XRD patterns of ZrB_2-B_4C-Mo ceramic composite sintered at different temperatures : (a) $1500^\circ C$, (b) $1600^\circ C$ and (c) $1800^\circ C$

4.2 Scanning Electron Microscopy:

4.2.1 SEM analysis of milled products

Fig.4.3 reveals that the SEM microstructure of ZrB_2-B_4C-Mo milled powders at different stages of milling (0 h (un-milled), 42 h and 60h). It is clearly evident from the figure that the micron size powder get reduces into sub-micron or nano-meter level with increase in milling time. It has been observed that initial size of particle is of ($<32\mu m$), due to the milling, particle size is reduced and become of size around $5-10\mu m$.

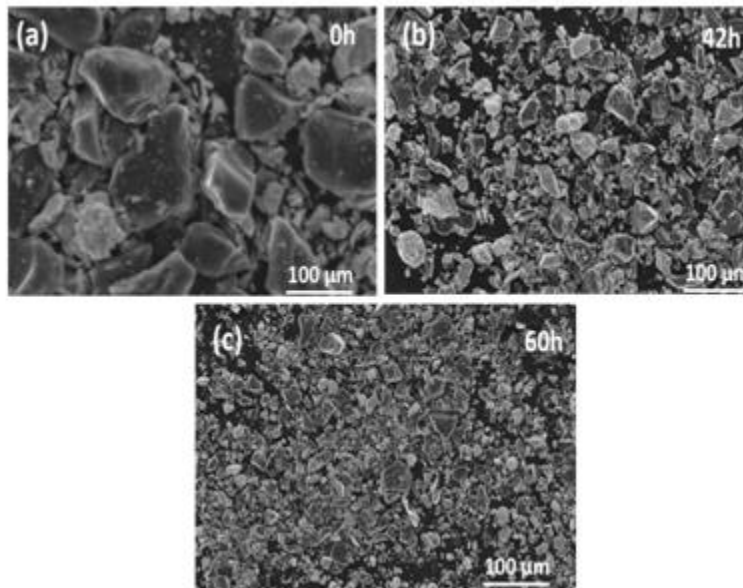


Fig 4.3: SEM Image of the milled powder of ZrB_2-B_4C-Mo at different milling times

4.2.2 SEM analysis of sintered products

Fig 4.4 shows that the SEM image of ZrB_2-B_4C-Mo composite sintered at $1500^\circ C$ in a tubular furnace in argon atmosphere for 3 hrs. It reveals that the partially sintering happen which confirms that the particles are not bonded properly. Similar kind of trends was found in the samples sintered at $1600^\circ C$ in conventional technique for 3 hrs which are shown in Fig 4.5. It is clear that in the second case, the percentage of sinterability is higher than that of samples sintered at $1500^\circ C$. As a result of that there is presence of porosity in the microstructures in both cases.

The partially sintered matrix this is due to that there the sintering temperature is not sufficient to make a strong bonding with the particles.

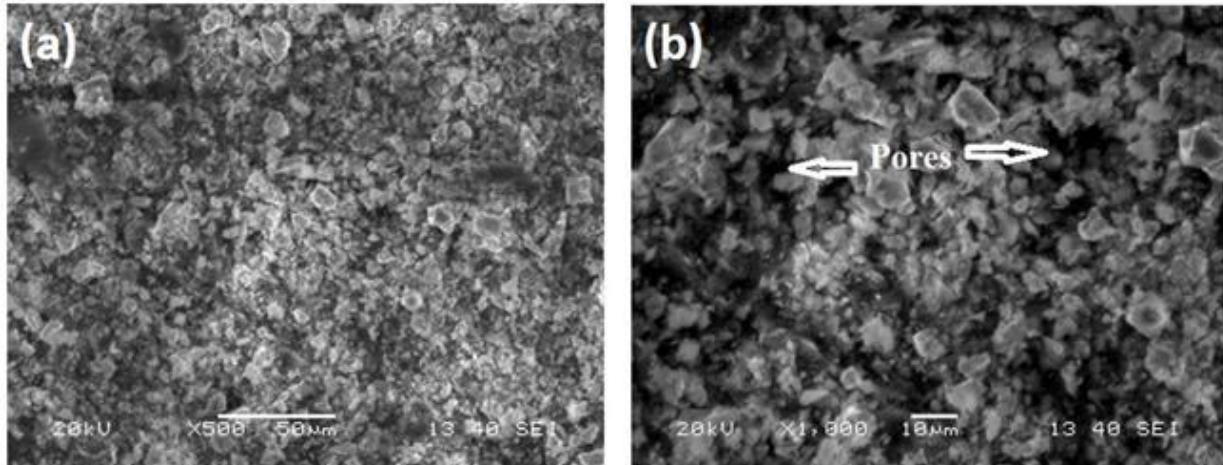


Fig 4.4: SEM Images of the sintered pellets of ZrB_2-B_4C-Mo at $1500^\circ C$: (a) lower and (b) higher magnifications.

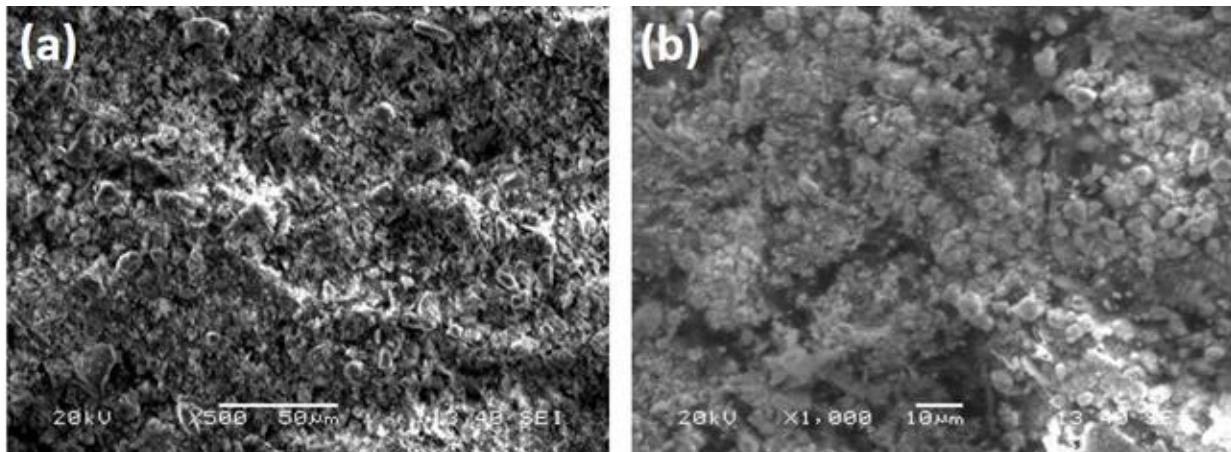


Fig 4.5: SEM Images of the sintered pellets of ZrB_2-B_4C-Mo at $1600^\circ C$: (a) lower and (b) higher magnifications.

The best results have been revealed during the sintering of ZrB_2-B_4C-Mo milled powder was done in plasma sintering technique. Fig 4.6 shows the microstructures of ZrB_2-B_4C-Mo composite sintered at $1800^\circ C$ in plasma sintering techniques for 30 sec-1min.. The figures reveal that the presence of bright phases i.e. ZrB_2 and dark phases i.e. B_4C in the microstructures of ZrB_2-B_4C-Mo sintered at $1800^\circ C$.

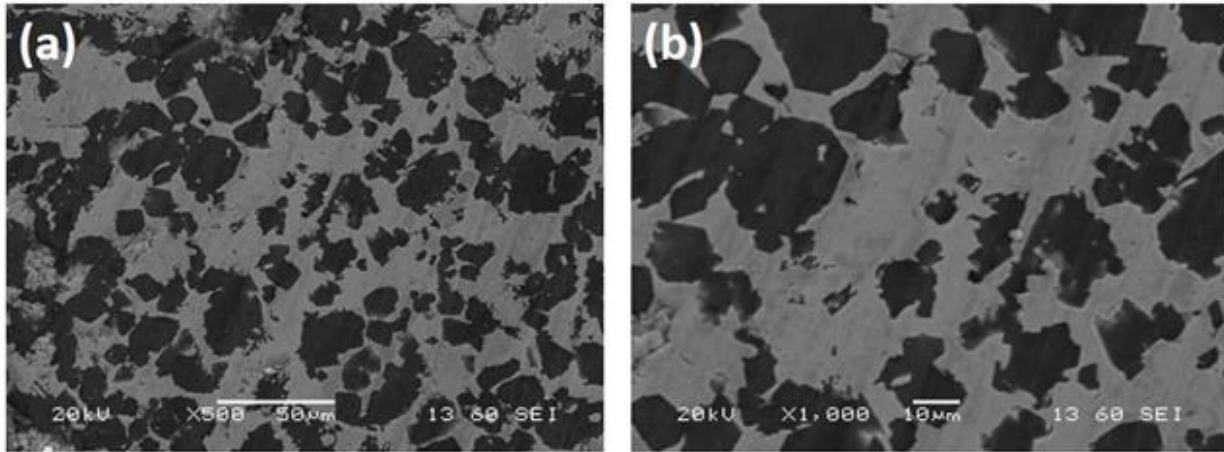


Fig 4.6: SEM images of ZrB₂-B₄C-Mo composite sintered at 1800°C by plasma sintering for different magnification : (a) low and (b) high

Fig 4.7 shows the microstructures of ZrB₂-B₄C-Mo composite sintered at 1800°C in plasma sintering techniques for 30 sec results some the area of pellete melted due to high localized heat generated by plasma. It reveals the dendritic microstructures where dark phase B₄C presence of interdendritic region of ZrB₂. As a result of that the percentage of sinterability increases rapidly and produce very high dense products as compare that of sample sintered at 1500 or 1600°C in conventional method.

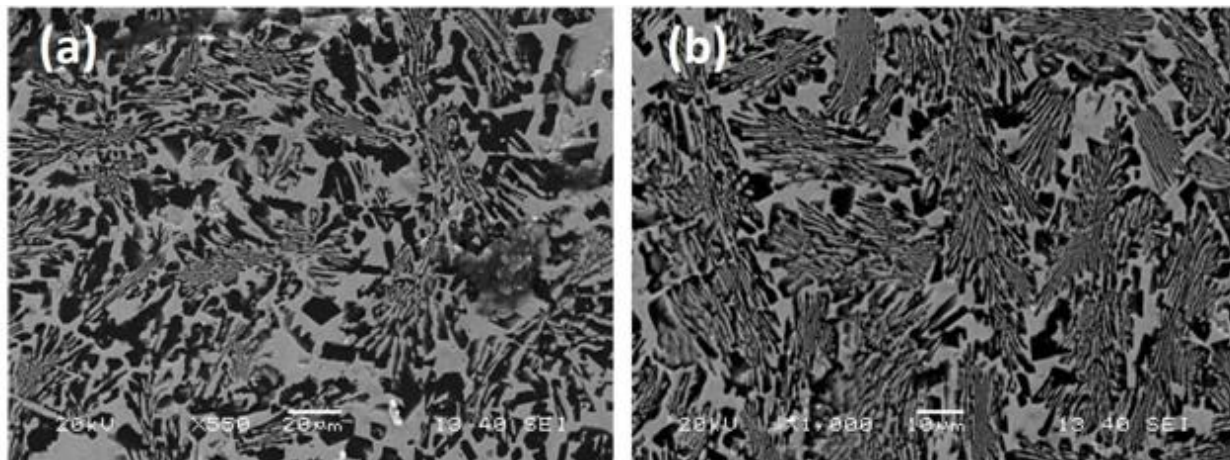


Fig 4.7: SEM images of melted region of ZrB₂-B₄C-Mo composite sintered at 1800°C by plasma sintering for different magnification: (a) low and (b) high showing dendritic structure.

4.3 Relative density/apparent porosity analysis:

It reveals that the samples sintered at 1500°C or 1600°C by conventional sintering method show lower density than that of samples sintered at 1800°C by plasma sintering method. It was observed that the samples sintered by conventional sintering showed incomplete sintering which results increase the amount porosity in the sintered products. But, samples sintered by plasma sintering with higher temperature has showed complete sintered and also some portion has been melted due to localized increase in temperature which results in increase in density of the sintered products.

It has been found that the bulk densities increase with fineness of the ZrB₂-B₄C-Mo composite mixture. Highest relative density achieved due to presence of ZrB₂ in the composite. The open-type porosity arises with increase in

B₄C content, but the amount of closed-type porosity shows a reverse behavior. Densification behavior of ZrB₂-B₄C-Mo composites has been improved remarkably by increasing sintering temperature by Spark plasma sintering technique, where temperature is in excess of 1800⁰C. With the progress of sintering process the nature of porosity changes gradually from open to closed form.

Therefore presence of negligible amount of open pores in ZrB₂-B₄C-Mo cermet verifies that spark plasma sintering is much fruitful than conventional sintering. By using finer starting powder particles by subsequent ball milling, intensified the elimination of voids, Solid state diffusion becomes more pronounced during sintering and finally leads to sealing off the open channels between particles by efficient mass transport between powder particles. As a result the relative density of the composite material milled 60 hrs will give rise to nearby theoretical density while sintering through spark plasma technique.

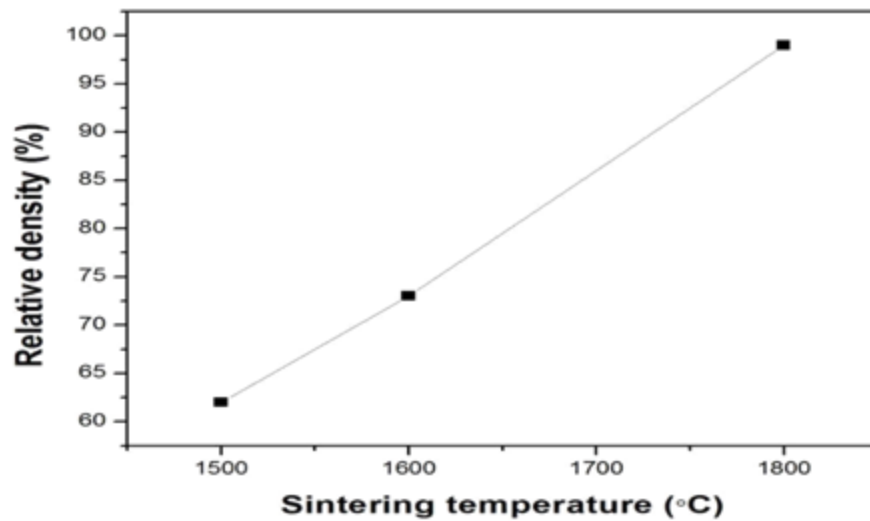


Fig. 4.8: Variation of density of ZrB₂-B₄C-Mo composites with function of sintering temperatures

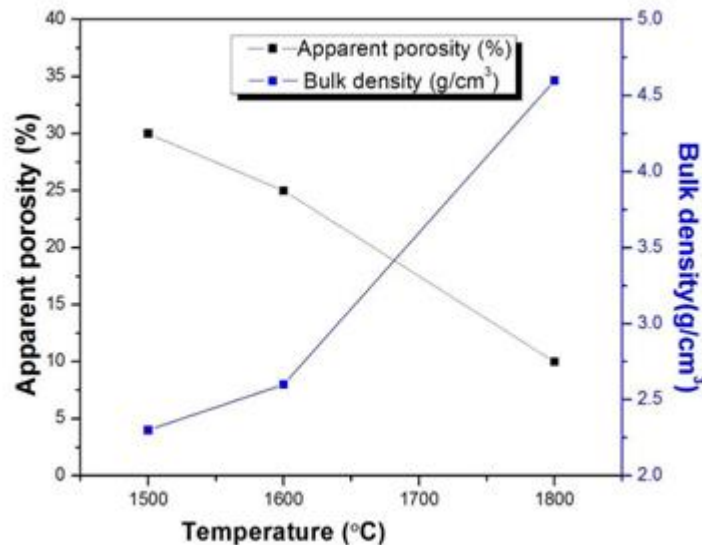


Fig. 4.9: The apparent porosity and bulk density of sintered ZrB₂-B₄C-Mo composite.

4.4 Vickers hardness Test:

Fig. 4.10 shows the variation of hardness of the ZrB₂-B₄C-Mo ceramic composites as the function of sintering temperatures. It is evident from the figure that the hardness value is linearly increases with increasing the sintering temperatures. The previous section we have discussed that the density of the sintered pellets increase with the increasing in sintering temperature and maximum density have been achieved of sample sintered at 1800°C in plasma sintering process. By the same logic the hardness value of sample sintered at 1800°C in plasma sintering process recorded maximum as compared to that of samples sintered at 1500°C or 1600°C.

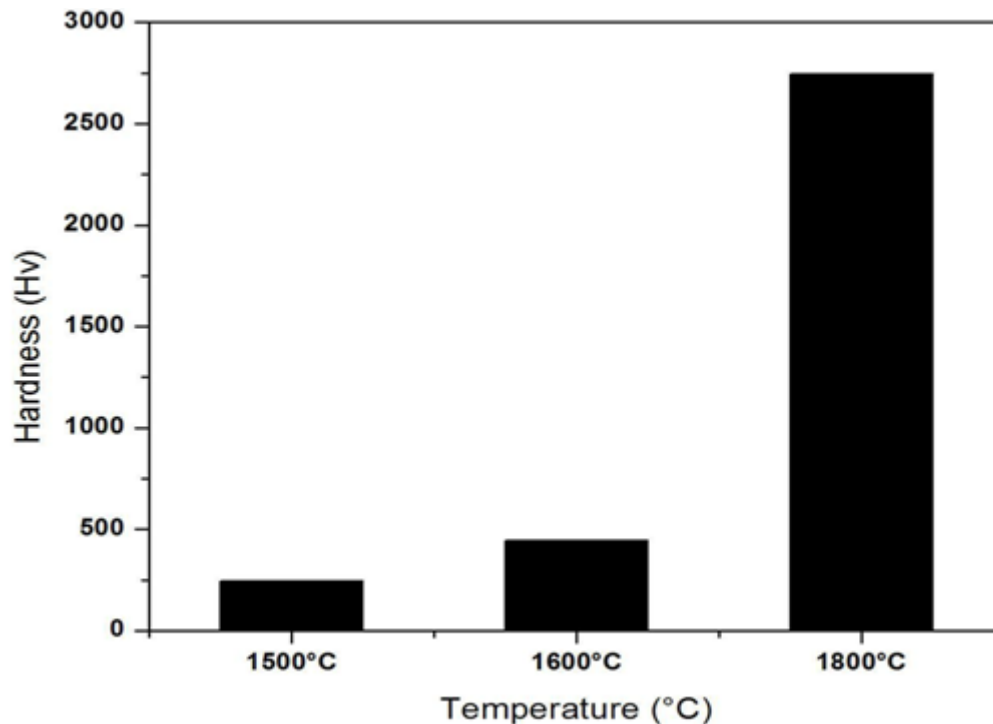


Fig. 4.10: Variation of hardness of sintered ZrB₂-B₄C-Mo composites with the function of sintering temperatures

The hardness results of all the sintered samples are summarized in Table 4.1. From table it is clear that hardness value increments with expanding sintering temperature because of faster diffusion at high temperature. As sintering temperature and milling time increases, bonding between particles improves and finally density and hardness increases.

From the graph (Fig. 4.12), the hardness of the composite increases from 234hv (2.3Gpa) to 2788hv (27.34Gpa) drastically, which was attributed to the decrease of porosity as the sintering temperature increased from 1600°C to 1800°C. Residual stresses in the sintered composite are another factor that may have contributed to the reduction in hardness. Since ZrB₂ has a hexagonal crystal structure with anisotropic thermal expansion coefficients ($6.88 \times 10^{-6} \text{ } ^\circ\text{C}^{-1}$) [29], grain growth of specimen could have produced micro-cracking during cooling as a result of residual stresses. Hence, micro-cracking due to the anisotropic thermal expansion behavior of ZrB₂ may have accounted for the lower hardness. In addition, B₄C has an average thermal expansion coefficient of ($5.25 \times 10^{-6} \text{ } ^\circ\text{C}^{-1}$) [29], which is lower than that of the ZrB₂-B₄C-Mo matrix. The thermal expansion coefficient mismatch between these individual elements could produce residual stresses near the ZrB₂-B₄C grain boundaries, which could also result in micro-cracking or lower hardness values as observed in case of sample sintered at 1500°C and 1600°C. A decrease of Vickers' hardness has been reported from the literature which gave the idea that conventionally sintered ZrB₂-B₄C ceramic base material showed lower hardness value due to the presence of residual stresses.

Higher densification value during spark plasma sintering due to formation of ZrC in the matrix as observed in XRD analysis observed in the material, which phenomena was not profound effect by analyzing XRD pattern in case of sample sintered at 1500°C and 1600°C.

Table 4.1: Relation between sintering temperature and hardness of sintered pellets

Sample	Sintering temperature (°C)	Vickers micro hardness(hv)
ZrB ₂ -B ₄ C-Mo ceramic matrix composite	1500	234
	1600	475
	1800	2788

It is cleared that the wear depth at 1500°C and 1600°C (in conventional sintering), was very much higher which are in the range of about 600-1400micron. But in spark plasma sintering, it was very much less (i.e. ~80micron). This may be due to liquid phase sintering Mo in the matrix during SPS and formation of ZrC and Mo₂BC which increases the hardness of the cermet as confirmed from XRD and SEM analysis. As a result of which matrix became stronger, intergranular and intragranular region became densified resulting less wear of the matrix of the cermet. But this effect was not observed upto some extend in case of cermet sintered at 1500°C and 1600°C.

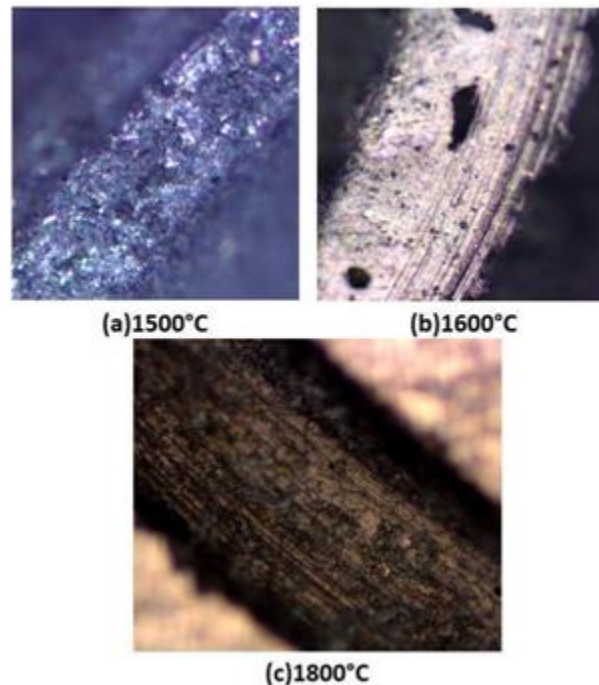


Fig 4.11: Optical microstructure of the worn surfaces of samples sintered at: (a) 1500°C, (b)1600°C and (c) 1800°C, respectively.

The sample after wear test showed some micro-crack and porous behavior in case of sintering at 1500°C and 1600°C (Fig4.11(a) and (b)). However such type of behavior was found nominally in case of sample sintered at 1800°C (Fig4.11 (c)). It is clear evident from the wear track thickness of sintered pellets at different temperatures that the increases of sintering temperature wear track thickness is decreases this is due to the fact that at high temperature (1800°C) the hardness of the composite is maximum.

V. CONCLUSIONS

In the present study, considerable effort has been done to develop ZrB₂-B₄C-Mo composites by mechanical alloying and conventional sintering and spark plasma sintering to determine the degree of enhancement in mechanical properties will be presented with detailed characterization of the microstructural evolution. A major effort in this work has been devoted to explore the various routes of consolidation with variation of sintering temperatures for developing bulk components retaining the novel microstructure obtained by mechanical alloying.

By evaluating the results in terms of synthesis and characterization, consolidation, physical properties (density and porosity) and mechanical properties (hardness and wear resistant property) in all the composites with variation of process parameters, the conclusions are presented. The conclusions emerging from the results presented and discussed in this chapter may be summarized as:

- Mechanical alloying is a potential route for synthesis of ZrB₂-B₄C-Mo composites powders.
- XRD analysis of the milled product show that in each composite produces solid solution indicating that ZrB₂, B₄C, Mo dissolve in course of high-energy ball milling for 60 h.
- SEM analysis show the degree of size reduction of powders is the function of the milling time. The measurement of the average particle size of after 60 h of milling product show the reduction in particle size in the range of 5-10µm.
- SEM analysis of sintered pellets confirms that the presence of bright phase of ZrB₂ and dark phase of B₄C in the matrix.
- Bulk physical properties (density and porosity) and mechanical properties (hardness and wear) for the present ZrB₂-B₄C-Mo composites are the function of sintering temperatures.
- Composites sintered at 1800°C by spark plasma sintering shows superior mechanical properties (hardness and wear). It records the harness value 27.34GPa (2788hv) as compared to the other composites sintered at lower temperature in conventional sintering technique.

Thus, the above results suggest that mechanical alloying followed by conventional sintering and spark plasma sintering are a flexible, convenient and promising route for synthesizing ZrB₂-B₄C-Mo composites with attractive mechanical properties. However, considering the entire spectrum of mechanical properties including hardness and wear, it is concluded that spark plasma sintering at 1800°C offers optimum combination of mechanical properties.

REFERENCE

1. Cutler RA. "Engineering properties of borides. In: Schneider SJ, editor. *Ceramics and glasses: engineered materials handbook*", vol.4. Materials Park, OH: ASM International; 1991. p. 787–803.
2. Mroz C. Zirconium diboride. *Am Ceram Soc Bull* 1995; 76:164–5.
3. Upadhyaya K, Yang JM, Hoffman WP. "Materials for ultrahigh temperature structure applications". *Am Ceram Soc Bull*, 1997; 58:51–6.
4. Norasethekul S, Eubank PT, Bradley WL, Bozkurt B, Stucker B, "Use of zirconium diboride copper as an electrode in plasma applications", *J Mater Sci* 1999;34:1261–70.
5. Levine SR, Opila EJ, Halbig MC, Kiser JD, Singh M, Salem JA. "Evaluation of ultra-high temperature ceramics for aero propulsion use", *J Eur Ceram Soc* 2002; 22:2757–67.
6. Zhu S, Fahrenholtz WG, Hilmas GE. "Enhanced densification and mechanical properties of ZrB₂-SiC processed by a pre ceramic polymer coating route", *Scripta Mater* 2008; 59:123–6.
7. Chamberlain AL, Fahrenholtz WG, Hilmas GE, Ellerby DT. "High-strength zirconium diboride-based ceramics", *J Am Ceram Soc* 2004; 87(6):1170–2.
8. Monteverde F, Bellosi A. "Development and characterization of metal-diboride based composites toughened with ultra-fine SiC particulates", *Solid State Sci* 2005; 5:622–30.
9. Wang HL, Wang CA, Yao XF, Fang DN. "Processing and mechanical properties of zirconium diboride-based ceramics prepared by spark plasma sintering", *J Am Ceram Soc* 2007; 90:1992–7.
10. Zhang XH, Qu Q, Han JC, Han WB, Hong CQ. "Microstructural features and mechanical properties of ZrB₂-SiC-ZrC composites fabricated by hot pressing and reactive hot pressing", *Scripta Mater*, 2008; 59:753–6.
11. Guo SQ, Kagawa Y, Nishimura T. "Mechanical behavior of two-step hot-pressed ZrB₂-based composites with ZrSi₂", *J Eur Ceram Soc*, 2009;29(4):787–94.

12. Tian WB, Kan YM, Zhang GJ, Wang PL, "Effect of carbon nanotubes on the properties of ZrB₂-SiC ceramics", *Mater Sci Eng A* 2008; 487:568–73.
13. Moya JS, Díaz M, Gutiérrez-González CF, Diaz LA, Torrecillas R, Bartolomé JF. Mullite-refractory metal (Mo, Nb) composites. *J Eur Ceram Soc* 2008;28:479–91.
14. Gu ML, Huang CZ, Zou B, Liu BQ, "Effect of (Ni, Mo) and TiN on the microstructure and mechanical properties of TiB₂ ceramic tool materials", *Mater Sci Eng A* 2006; 433:39–44.
15. Deng Jianxin, Sun Junlong, "Microstructure and mechanical properties of hot-pressed B₄C/TiC/Mo ceramic composites," *Ceramics International*, vol.35, pp.771–778, 2009.
16. XinYan Yue, ShuMao Zhao, Peng Lü, Qing Chang, HongQiang Ru, "Synthesis and properties of hot pressed B₄C–TiB₂ ceramic composite", *Materials Science and Engineering A*, vol. 527, pp. 7215–7219, 2010.
17. I. Topcu, H.O. Gulsoy, N. Kadioglu, A.N. Gulluoglu, "Processing and mechanical properties of B₄C reinforced Al matrix composites," *Journal of Alloys and Compounds*, vol.482, pp.516-521, 2009.
18. Han Wenbo, , Gao Jiaying, Zhang Jihong, Yu Jiliang, "Microstructure and Properties of B₄C-ZrB₂ Ceramic Composites" *International Journal of Engineering and Innovative Technology (IJEIT)*,vol 3,pp.163-166,2013.
19. Choe H, Chen D, Schneibel JH. "Ambient to high temperature fracture toughness and fatigue-crack propagation behavior in a Mo-12Si-85B (at.%) Intermetallic", *Intermetallic* 2001;9(4):319–29.
20. Bartolomé JF, Díaz M, Requena J, Moya JS, Tomsia AP. Mullite/molybdenum ceramic-metal composites. *Acta Mater* 1999; 47:3891–9.
21. Wang K, Robert RR. "The role of defects on thermophysical properties: thermal expansion of V, Nb, Ta, Mo and W", *Mater Sci Eng R* 1998;23:101–37.
22. C. Suryanarayana, Nasser Al-Aqeeli "Mechanically alloyed Nano composites", *Progress in Materials Science*, vol 58, 2013, pp 383–502.
23. Chawla KK, "Composite materials science and engineering", 3rd ed. 2009, New York: Springer;.
24. Sumin Zhu, William G. Fahrenholtz, Gregory E. Hilmas, Shi C. Zhang, Edward J. Yadlowsky, Michael D. Keitz "Microwave sintering of a ZrB₂–B₄C particulate ceramic composite" *Composites volume 39* , 2008,pp 449–453
25. Hailong Wang, Deliang Chen, Chang-An Wang, Rui Zhang, Daining Fang , " Preparation and characterization of high-toughness ZrB₂/Mo composites by hot-pressing process" *Int. Journal of Refractory Metals & Hard Materials*, vol 27 ,2009),pp 1024–1026
26. S.G. Huang*, K. Vanmeensel, J. Vleugels "Powder synthesis and densification of ultrafine B₄C-ZrB₂ composite by pulsed electrical current sintering" *Journal of the European Ceramic Society*, vol 34 , 2014,pp 1923–1933.
27. Mahsa Jalal Mousavi, Mohammad Zakeri , Mohammad reza Rahimpour , Elham Amini "Mechanical properties of pressure-less sintered ZrB₂ with molybdenum, iron and carbon additives" *Materials Science & Engineering* vol 13,2014,pp 3–7.
28. R.V. Krishnaraon, Md.Zafir Alam, Dipak Kumar Das, V.V. Bhanu Prasad "Synthesis of ZrB₂–SiC composite powder in air furnace" *Ceramics International*, vol 40, 2014, pp15647–15653
29. Mehdi Shahedi Asl, Mahdi Ghassemi Kakroudi, Behzad Nayebi "A fractographical approach to the sintering process in porous ZrB₂–B₄C binary composites" *Ceramics International*, 2014.
30. Caen Ang, Aaron Seeber, Kun Wang, Yi-Bing Cheng " Modification of ZrB₂ powders by a sol–gel ZrC precursor—A new approach for ultra-high temperature ceramic composites" *Journal of Asian Ceramic Societies*, vol-1, 2013,pp 77–8.